Pseudomonas silesiensis sp. nov. strain A3^T isolated from a biological pesticide sewage treatment plant and analysis of the complete genome sequence.

Michał A Kaminski[1], Ewa M Furmanczyk[1], Adam Sobczak[1,2], Andrzej Dziembowski[1,2], Leszek Lipinski[1,*]

[1]Institute of Biochemistry and Biophysics, Polish Academy of Sciences, Warsaw, Poland

[2]Institute of Genetics and Biotechnology, Faculty of Biology, University of Warsaw, Warsaw, Poland

* Corresponding author at: Institute of Biochemistry and Biophysics, Polish Academy of Sciences, Pawinskiego 5a, 02-106 Warsaw, Poland

E-mail address: lechu@ibb.waw.pl (L. Lipinski)

Abstract

Microorganisms classified in to the *Pseudomonas* genus are a ubiquitous bacteria inhabiting variety of environmental niches and have been isolated from soil, sediment, water and different parts of higher organisms (plants and animals). Members of this genus are known for their metabolic versatility and are able to utilize different chemical compounds as a source of carbon, nitrogen or phosphorus, which makes them an interesting microorganism for bioremediation or bio-transformation. Moreover, *Pseudomonas sp.* has been described as a microorganism that can easily adapt to new environmental conditions due to its resistance to the presence of high concentrations of heavy metals or chemical pollution. Here we present the isolation and analysis of *Pseudomonas silesiensis* sp. nov. strain A3^T isolated from peaty soil used in a biological wastewater treatment plant exploited by a pesticide packaging company. Phylogenetic MLSA analysis of 4 housekeeping genes (16S rRNA, *gyrB*, *rpoD* and *rpoB*), complete genome sequence comparison (ANIb, Tetranucleotide identity, digital DDH), FAME analysis, and other biochemical tests indicate the A3^T strain (type strain PCM 2856^T =DSM 103370^T) differs significantly from the closest relative species and therefore represents a new species within the *Pseudomonas* genus. Moreover, bioinformatic analysis of the complete sequenced genome

showed that it consists of 6,823,539 bp with a 59.58 mol% G+C content and does not contain any additional plasmids. Genome annotation predicted the presence of 6,066 genes, of which 5,875 are coding proteins and 96 are RNA genes.

Keywords:

Pseudomonas – Soil – Pesticide – Wastewater Treatment Plant – Complete Genome Sequence – Complete Genome Assembly

Abbreviations:

ANIb - Average Nucleotide Identity based on BLAST; COG - Clusters of Orthologous Groups; DDH - DNA-DNA Hybridization; FAME - Fatty Acid Methyl Esters; MIGS - Minimum Information about a Genome Sequence; MLSA - Multilocus Sequence Analysis; PHA – polyhydroxyalkanoate; PHB – polyhydroxybutyrate

Introduction

Pseudomonas is a bacterial genus comprised of pathogenic and non-pathogenic Gram-negative microorganisms able to colonize different niches such as living organisms (both plants and animals), soil, sediment and water. The *Pseudomonas* genus is highly diverse and has been reclassified several times as new methods for classification have appeared [1]. It is now accepted that it is divided into *Pseudomonas fluorescens* and *Pseudomonas aeruginosa* lineages. Among them, several groups and subgroups can be distinguished as was previously proposed by Mulet M et al. [2] and Garrido-Sanz D et al. [3]. However, many identified *Pseudomonas* isolates are not classified at the species level.

As members of this genus demonstrate ease of culture *in vitro,* combined with huge metabolic diversity, they have many applications in biotechnology and industry. One of the most well-studied members is *Pseudomonas putida*, which was found to be easy for genetic engineering and thus useful for scientific studies as well as for a vast number of industrial applications. Strains of *P. putida* proved to be useful for synthesis and production of bio-based materials, chemical and pharmaceutical compounds [4–6]. Metabolic properties of *P. putida* and many other members of *Pseudomonas* genus were widely used for biotransformation of a broad portfolio of compounds [7–9]. It is also known that long-term exposure imposed on bacteria in the environment forces the development of metabolic mechanisms to cope with toxic xenobiotics deposited mainly by human activity. This feature of different *Pseudomonas* strains isolated from sites of high chemical pollution were used for bioremediation of soil, water and sediment contaminated with oil, heavy metals, phenolics, detergents, dyes, and pesticides [10–13].

Among the previously mentioned factors, pesticides constitute a specific type of contamination due to the fact that they are intentionally released into the environment in large quantities. The highest pesticide contamination levels have been reported in the areas surrounding pesticide production and packaging [14,15]. In these sites pesticides were spread by inappropriate management of water used by the industry for installation and maintenance [16,17]. To minimize the negative impact of industrial sewage, some locations were equipped with biological wastewater treatment plants where peaty soil was used to filter dangerous contamination. This study describes the isolation of

Pseudomonas silesiensis strain A3^T from one such wastewater treatment plant utilized by a pesticide packaging company in operation since 1986 in Jaworzno City (Poland). Phylogenetic analysis of partial sequences of 16S rRNA, *gyrB*, *rpoD* and *rpoB* genes indicates this strain belongs to the *Pseudomonas mandelii* subgroup within the *Pseudomonas fluorescens* group [2]. Species belonging to this subgroup were previously isolated from natural mineral water [18–20], rhizospheric soil [21], arsene contaminated desert sediments [22] and PCB and tar-polluted soil [23,24]. Genome sequencing of *Pseudomonas silesiensis* strain A3^T and bioinformatic analysis gave insight into the possible application of this new strain for either bioremediation of chemically contaminated soil or pollutant biotransformation.

Materials and methods

Sample collection and bacteria isolation

Pseudomonas silesiensis sp. nov. strain A3^T was isolated from peaty soil used to fill tanks from a biologic wastewater treatment plant used by a pesticide manufacturer in Jaworzno City (Silesia district, south western Poland). The sample was taken from a depth of 5-30 centimeters at a distance of 5 meters from the inlet valve of the pesticide-contaminated water. 5 kg of soil was collected, homogenized, and sieved with ¼" and 1/16" sieves. For bacteria isolation, soil samples were placed in plastic bags and stored at 8°C until isolation. 10 g of soil was transferred to a Waring blender, then 100 mL of 0.9% NaCl was added. The sample was homogenized three times for one minute, with one minute pauses for cooling on ice. After 5 minutes of decantation, the supernatant was collected. The procedure was repeated three times resulting in a total volume of 300 mL of bacteria in suspension. Bacteria were centrifuged for 10 minutes at 5000 x g and re-suspended in 500 µL of saline. Dilutions 10^{-3}, 10^{-4} and 10^{-5} were plated in triplicates on soil extract agar plates (described below). After 7 days of incubation in 23°C, colonies of different morphologies and size were transferred to 96-well plates and stored at -80°C. In total 238 colonies were isolated, which belonged mainly to *Pseudomonas* sp., *Flavobacterium* sp., *Variovorax* sp. and *Stenotrophomonas* sp.. Soil extract was made by sterilization of 500 g of air-dried garden soil in 1 L of distilled water for one hour at 121°C. Afterwards, solid

particles were centrifuged for at least 10 minutes, and the resulting extract was used for the experiments. Agar plates were made by the addition of agar to 1.5% (final concentration).

Growth conditions and genomic DNA preparation

For genomic DNA isolation, the strain was inoculated into 50 mL of liquid LB medium and cultivated overnight at 23°C in a shaker at 150 rpm. The overnight culture was centrifuged and suspended in 10 mL of 2x diluted lysis buffer [25] supplemented with 2 mg/mL lysozyme and 500 U/mL of achromopeptidase and incubated at 37°C for 1 h. Then, 50 µL of proteinase K (40 mg/mL) was added followed by a 30 min incubation at 37°C. The final cell lysis step was carried out with the addition of an SDS solution to a final concentration of 2% followed by a 2 h incubation at 55°C. DNA extraction was performed using a standard phenol-chloroform protocol. The amount and quality of isolated DNA was verified using the NanoDrop 2000c Spectrophotometer, Qubit 2.0 Fluorimeter and gel electrophoresis.

16S rRNA and Multilocus Sequence Analysis (MLSA)

For 16S rRNA gene phylogenetic analysis, the type strains of closely related species were included in the alignments. Alignments were prepared using ClustalW and the analysis was performed using the maximum-likelihood method and the Tamura-Nei model. All positions containing gaps or missing data were eliminated, which resulted in a 1,271 bp sequence in the final dataset. Bootstrap analysis of 1,000 replicates was performed to evaluate the phylogenetic tree topology. MLSA analysis was performed with additional partial sequences from the *gyrB, rpoD* and *rpoB* genes. Reference sequences of type strains were downloaded from the PseudoMLSA database [26] or directly from NCBI database (www.ncbi.nlm.nih.gov). All accession numbers of genes and genomes sequences used in this study are presented in **Supplementary tables 1** and **2**. Type strain information was carefully checked according to information available on websites of microorganism collections. Alignments for each gene were performed separately using ClustalW, and the longest common fragments identified were selected for analysis. This process resulted in the following sequence

lengths: 16S rRNA – 1,313-1,316 bp, *gyrB* - 534-539 bp, *rpoD* - 616-622 bp and *rpoB* – 852 bp. Next, sequences were concatenated in the following order: *16S-gyrB-rpoD-rpoB.* This realignment resulted in a sequence that was 3,345 bp long. Phylogenetic analysis was performed using the MEGA software version 6.0 [27], the maximum-likelihood method and the Tamura-Nei model [28]. All positions containing gaps or missing data were eliminated, which resulted in a 3,254 bp sequence in the final construct. Bootstrap analysis of 1,000 replicates was performed to evaluate the phylogenetic tree topology.

Biolog and API20NE analysis

Plate test analysis was performed using the Biolog System using GENIII microplates. Tests were performed at 30°C, according to the manufacturers' instructions. Biolog test was additionally supplemented with API 20NE stripe test. All tests were inoculated with cells pre-grown on LB medium and diluted with relevant inoculation medium. Biolog plates and API 20NE stripes were evaluated after 48 h of incubation. *P. silesiensis* A3^T was tested simultaneously with closely related type strains: *P. frederiksbergensis* DSM 13022^T (=CIP 106887^T), *P. lini* DSM 16768^T (=CCUG 51522^T =CIP 107460^T =CFBP 5737^T), *P. arsenicoxydans* DSM 217171^T (=CECT 7543^T) and *P. mandelii* DSM 17967^T (=LMG 21607^T =CIP 105273^T).

Chemotaxonomic analysis

Analysis of cellular fatty acid composition was performed at the Leibniz Institute DSMZ using the Sherlock Microbial Identification System (MIDI, Microbial ID, Newark DE 19711 USA). Peaks were automatically integrated and fatty acid names and percentages were calculated by the MIS Standard Software (Microbial ID, Sherlock version 6.1, database TSBA40 4.10). Analysis of *P. silesiensis* A3^T and closely related type strains was performed on microbial cells grown for 48 h in 23°C on LB medium.

Other phenotype tests

Flagellation of bacteria was verified under an optical microscope after flagella staining according to the protocol by Heimbrook et al. [29]. Production of fluorescein was tested on King B medium after 24 h of incubation. The ability to accumulate polyhydroxyalcanoic acids was assessed with the Nile Red staining method [30]. Starch hydrolysis was verified on 0.5% starch agar plates after 24 h of growth by adding iodine solution around growing colonies. Casein hydrolysis test was carried out on casein-skim milk agar plates and verified by the creation of a clear zone on the plate around the colony. The same procedure was used for lipase activity verification by the tributyrin degradation test on agar plates supplemented with 0.1% tributyrin. Resistance to ampicillin was tested on LB agar plates with an ampicillin concentration in range 50-400 μg/mL. Oxidase test was performed using commercial discs purchased from Sigma-Aldrich (Cat. No. 70439). Salt tolerance was examined by bacteria growth in LB medium with an NaCl concentration in the range 0-6%. All tests were performed at 23°C.

Genome sequencing and assembly

Three libraries were prepared for genome sequencing: 1) a paired-end library with an insert size of 500 bp, 2) a Nextera® Mate Pair library with an average insert size of 8 kb, and 3) a Lucigen NxSeq® Long Mate Pair library with an average insert size of 20 kb. Sequencing was performed on the Illumina MiSeq platform with a 300 bp read length resulting in 754,929, 1,443,756 and 3,674,976 raw paired reads respectively. Next, a number of bioinformatics tools were used to analyze the raw reads. Adapters from the raw reads were trimmed using Cutadapt [31], and quality filtered with Sickle [32] (quality at least Q30). The mate-paired libraries were also processed using specific scripts provided by the manufacturer. After all pre-processing steps, average genome coverage was estimated at ~95x. Assembly was performed using the SPAdes 3.6.2 software [33] which produced two scaffolds. Remaining gaps in the scaffold sequences were filled manually using a PCR reaction and Sanger sequencing.

Genome annotation

The genome was annotated using the NCBI Prokaryotic Genome Annotation Pipeline [34]. Genes with signal peptides were identified with SignalP 4.1 [35], and genes with transmembrane helices were identified by aligning ORFs to the Transporter Classification Database (TCDB) [36]. The complete genome sequence was deposited in GenBank under accession number CP014870.1 and the genome project was deposited in the Genomes OnLine Database under Gp0137126.

Results and discussion

Organism information, classification and biochemical features

Bacterial colonies isolated from peaty soil and grown on LB-agar plates were a round shape, had a smooth surface and edges and a milky-yellow color (**Figure 1A**). Cell morphology and the type of flagellation analysis based on electron or optical microscopy and the wet-mount staining technique [20] show that the *P. silesiensis* strain A3^T is Gram negative, rod-shaped with PHA granules inside, and motile by one polar flagellum (**Figures 1B and 1C**). Bacterial cell movement characteristic of this type of motion was observed under optical microscope. Detailed classification and isolation features are presented in **Table 1.**

A similarity search with the full-length nucleotide sequence of the 16S rRNA gene (deposited in GenBank under accession number KX276592) performed with EzBioCloud [37] alignment indicated 99.93% identity with *Pseudomonas mandelii* CIP 105273^T, 99.52 with *Pseudomonas frederiksbergensis* JAJ28$^{T\ T}$, and 98.45% with both *P. tremae* CFBP 3225^T and *P. cannabina* CFBP 2341^T. As it can also be seen in **Figure 2** strain A3^T groups within species belonging to the *P. fluorescens* group and *P. mandelii* subgroup according to the classification proposed by Mulet et al. 2010 [2]. However, analysis based on 16S rRNA sequence is not sufficient for species assignment within the *P. fluorescens* group. The identity of concatenated 16S rRNA, *gyrB*, *rpoD* and *rpoB* genes between the A3^T strain and other type strains of the *P. mandelii* subgroup is represented as follows: *P. lini* CCUG 51522^T and *P. mandelii* CIP 105273^T (97.5%), *P. arsenicoxydans* CECT 7543^T and *P. frederiksbergensis* DSM 13022^T (97.2%) and *P. migulae* CCUG 43165^T (96.9%). The above

mentioned MLSA results confirmed the assignment of the A3^T strain to the *P. mandelii* subgroup, which is in agreement with previous studies, as the identity values between species inside this particular subgroup oscillate around the mean value of 97.93% [2]. Strain A3^T represents a separate branch on the phylogenetic tree with 41% bootstrap support (**Figure 3**). The same structure of tree topology was obtained using only *gyrB*, *rpoD* and *rpoB* genes excluding 16 rRNA gene sequence as presented in **Supplementary Figure 1**.

At the time of writing only three genomes from closely related species (according to MLSA results) were available in public databases: *P. mandelii* LMG 21607^T (=DSM 17967^T =CIP 105273^T), *P. lini* DSM 16768^T (=CCUG 51522^T =CIP 107460^T =CFBP 5737^T) and *P. arsenicoxydans* CECT 7543^T (=VC-1^T =DSM 27171^T). Thus, genomes of *P. tremae* ICMP 9151, *P. cannabina* ICMP 2823^T and *P. meliae* CFBP 3225^T, were included additionally in the analysis as they represented high similarity of 16S rRNA gene sequence. This genomes were analyzed with ANIb and Tetra tests using JspeciesWS [38] and digital DDH analysis using the DSMZ GGDC platform [39] (**Table 2**). The highest ANIb and digital DDH values were 86.31% and 34.50% for *P. mandelii* LMG 21607^T, respectively. It can be seen that strains of species *P. tremae*, *P. cannabina* and *P.meliae* are distant relatives in spite of high identity of 16S rRNA sequence. Both, ANIb and digital DDH values were below the species cut-off threshold (95% and 70% respectively). Also the tetra z-score with the value 0.98344 is very low. The above comparison of several available genomes of type strains, indicated that *P. silesiensis* A3^T should be considered as a separate species.

The phenotypic characteristics (Biolog and API20NE analysis) of described here strain provide further support for its classification as a novel species. The *P. silesiensis* A3^T features are reported below, and the differences with respect to the close related *Pseudomonas* representatives are collected in **Table 3** and **Table 4**.

Results from Biolog GENIII MicroPlate, allowed to distinguish the *P. silesiensis* A3^T from all analyzed closely related species by the lack of oxidation of N-Acetyl-D-Glucosamine. Strain A3^T showed the lowest tolerance to salinity, as in Biolog test it does not give positive results in presence of

4% and 8% NaCl as the other species, whereas it is able to grow in 4% NaCl in LB medium as indicated in Table 3. It is also sensitive to minocycline. It gives negative results for myo-inositol oxidation as *P. arsenicoxydans* DSM 217171^T. It can be distinguished from *P. arsenicoxydans* DSM 217171^T by D-trehalose assay which is positive for the A3^T strain. It also can be differentiated from *P. arsenicoxydans* DSM 217171^T and *P. mandelii* DSM 17967^T with a positive sucrose test. *P. silesiensis* A3^T, the same as *P. lini* DSM 16768^T is sensitive to lithium chloride and gives negative results in Biolog test. Moreover, *P. frederiksbergensis* DSM 13022^T can be distinguished by the ability to oxidize inosine and D-sorbitol.

Considering the results from the API 20NE test *P. silesiensis* A3^T can be differentiated from all type strains analyzed in this study with the inability to assimilate N-acetyl-glucosamine (result confirmed with Biolog) and trisodium citrate. It differs from *P. frederiksbergensis* DSM 13022^T, *P. lini* DSM 16768^T and *P. mandelii* DSM 17967^T with the ability to assimilate D-maltose, the same as *P. arsenicoxydans* DSM 217171^T. *P. silesiensis* A3^T as well as *P. lini* DSM 16768^T and *P. mandelii* DSM 17967^T reduce nitrates to nitrites, *P. frederiksbergensis* DSM 13022^T reduces nitrates to nitrogen, whereas *P. arsenicoxydans* DSM 217171^T is unable to reduce nitrates at all.

The FAME analysis showed that the major fatty acids present in the bacteria were summed feature 3 of unseparated $C_{16:1\ \omega7c}$ and $C_{15:0\ ISO\ 2OH}$ (37%), $C_{16:0}$ (28%) and $C_{18:1\ \omega7c}$ (18%). There were also fatty acids in lower amounts as $C_{12:0}$ (6%), $C_{10:0\ 3OH}$ (4%), $C_{12:0\ 3OH}$ (3%), and $C_{12:0\ 2OH}$ (1%). This result is in agreement with the common composition of fatty acids in *Pseudomonas sp*. [40].

Comparison of selected features between *Pseudomonas silesiensis* A3^T and other closely related species representing different type strains is presented in **Tables 3** and **4**. A more detailed comparison is presented in **Supplementary tables 3** and **4**.

Genome sequencing results

General genome properties

Genome statistics are presented in **Table 5** and identity comparison between genomes of *P. mandelii* LMG 21607^T, *P. lini* DSM 16768^T and *P. arsenicoxydans* CECT 7543^T is visualized in **Figure 4**. It can be seen that it contains regions not identified in the other genomes with a significantly lower GC content, which was likely acquired by horizontal gene transfer. The size of the complete genome is 6,823,539 bp. The genome contains 59.58 mol% G+C content as determined from the complete genome sequence and is 83.45% coding. It is composed of one circular chromosome and does not contain any plasmid sequences. The total number of predicted genes is 6,066, of which 5,875 (96.85%) are proteins coding genes and 78.99% have assigned a putative function, while the remaining 21.01% have no assigned function. The *P. silesiensis* A3^T genome has 96 RNA genes: 71 tRNA, 1 tmRNA, 21 rRNA (7 rRNA clusters) and 3 ncRNA. Assignment of genes into COG (Clusters of Orthologous Groups) functional categories for *P. silesiensis* A3^T in comparison with *P. mandelii* LMG 21607^T, *P. lini* DSM 16768^T and *P. arsenicoxydans* CECT 7543^T did not show any significant differences. These results are presented in **Table 6**.

Analysis of the genome sequence

Analysis of the complete and circularized genome of new bacteria strains usually gives broad information about microorganism metabolism and its biochemical features. Detailed analysis of fully sequenced and circularized *P. silesiensis* A3^T strain sheds some light into this microorganism's biology.

As API 20NE test showed, the A3^T strain exhibits the ability to reduce nitrate to nitrite. The incomplete denitrification occurs despite the presence in the A3^T genome gene clusters coding enzymes responsible for the entire denitrification process. This observation needs to be further investigated especially in the context that the gene clusters identified in *P. silesiensis* strain A3^T show a high similarity to the clusters described previously in denitrifying *Pseudomonas fluorescens* F113 [41].

Accumulation of polyhydroxyalkanoate (PHA) or polyhydroxybutyrate (PHB) inside of cytoplasmic granules was previously observed for a variety of microorganisms, and this process enhances the survival and fitness of cells [42]. Among *Pseudomonas* species, the closest relative of strain A3^T is *P. mandelii* CBS-1, that has been previously described as a microorganism exhibiting PHB producing features [43]. Transmission electron microscope analysis and Nile Red staining of the A3^T strain, showed presence of characteristic granules in the cells **(Figure 1C)**, which suggested ability for PHA or PHB synthesis. The A3^T strain genome revealed two loci harboring genes assigned to the polyhydroxyalkanoate synthesis pathway, which likely indicates that granules present in the cytoplasm of the A3^T strain will contain PHA. The first gene cluster is composed of *phaB-phaA-phaC* related genes encoding Acetoacetyl-CoA reductase (PMA3_13890), Acetyl-CoA acetyltransferase (PMA3_13885), and Class I poly(R)-hydroxyalcanoic acid synthase (PMA3_13880). Upstream from the *pha* cluster there is also an ORF encoding Phasin - protein associated with PHA granule formation (PMA3_13905) and a transcriptional regulator (PMA3_13895). This gene cluster shares high similarity to class I clusters present in other *Pseudomonas* species [44]. However, the second *pha loci* has a genetic structure of class II and is composed of 6 genes: *phaC1-phaZ-phaC2-phaD-phaF-phaI* (ORF's PMA3_01425-01400).

Production of different exopolysaccharides is known to play a crucial role in microorganism survival in highly contaminated environments [45]. According to the genomic features identified, the *P. silesiensis* strain A3^T may be also able to synthetize cellulose due to the presence of a set of *bcsEFGRQABZC* genes which belong to the type IIb operon structure [46] (PMA3_00380-PMA3_00340). Also, 12 *alg* genes responsible for alginate production and secretion were identified in the genome (PMA3_24585-PMA3_24640).

Moreover, several secretion systems were identified in the genome of the A3^T strain. The Type 1 Secretion System (T1SS) is present in three copies, and two of the *tolC* genes function as orphan genes. The identified T2SS-like structure is present in only one copy and does not share a high similarity to the previously described T2SS. The T2SS structure in the A3^T strain is divided into 3 *loci*.

The first *loci* consists of 8 genes (PMA3_17620-17585), of which 3 resemble *xcpQRZ* genes, one is a *pilN* gene, two are annotated as the type II protein secretion protein precursor likely encoding minor pseudopilins (XcpU or XcpW), and two are genes of unknown function. The second *loci* is composed of two genes similar to *xcpTS* (PMA3_17665 and PMA3_17670). Prepilin signal peptide peptidase gene *xcpA* is encoded by the third *loci* (PMA3_03385-03410). This gene located within the cluster containing *xcpRS* genes and the *pilA* gene encoding fimbrial protein precursor. Additional genes identified at this *loci* include Dephospho-CoA kinase CoaE and the DNA gyrase inhibitor YacG. No similar homologues of genes encoding XcpPXY protein were identified. Also, there were two T5SS (PMA3_14935-14940 and PMA3_27465) and two T6SS secretion systems identified (PMA3_10530-10610 and PMA3_11270-11400) in the $A3^T$ strain genome.

As mentioned previously, bacterial cell movement observed under optical microscope and wet-mount staining suggests presence of flagellar structures in the cell surface. Additionally, prediction of *in silico* transcriptional units using Pathway-tools [47] identified flagellar protein coding genes which were grouped as follows: *flgA-flgBCDE-flgF-flgG-flgHIJKL-fliC-flaG-fliD-fliS-fleQ-fliEFGHIJ-fliK-fliLM-fliNOPQR-flhB-flhAF.* Dashes represent predicted separate transcriptional units. It is also worth mentioning that *flgBCDE* genes were in *loci* separate from the rest of the *flg* genes, which is considered unusual for *Gammaproteobacteria* [48].

Several genomic islands were predicted using IslandViewer software [49]. One island was 34 kb long and had 8% lower G+C content in comparison to the complete genome. From 24 ORF present in this putative island there were 9 assigned as hypothetical proteins. However, the toxin-antitoxin system RelBE (PMA3_26835 and PMA3_26840) was correctly identified as well as the probable type III restriction-modification system associated with the methyl-accepting chemotaxis protein and ATP-dependent helicase (PMA3_26815, PMA3_26820, PMA3_26825 and PMA3_26830). Moreover, the genomic island sequence also contained the following prophage regulatory proteins: S24_LexA-like regulatory protein (PMA3_26720), Prophage CP4-57 Bacteriophage P4 integrase (PMA3_26725), YqaJ-like viral recombinase (PMA3_26750), IS2 repressor TnpA (PMA3_26800) and IS2 transposase

TnpB (PMA3_26805). These results suggest that this genomic island could originate from a prophage or cryptic prophage sequence.

Conclusions

According to the genomic sequence, *Pseudomonas silesiensis* strain A3^T appears to be a versatile bacterium with potential biotechnological and ecological applications including pesticide-contaminated soil bioremediation and the production of biodegradable polyhydroxyacids or natural biosurfactans. On the basis of phenotypic, phylogenetic and genomic analyses, we formally propose the creation of *Pseudomonas silesiensis* sp. nov. that contains strain A3^T. In this study we provide a phenotypic and biochemical characterization of *Pseudomonas silesiensis* sp. nov. strain A3^T.

Description of *Pseudomonas silesiensis* sp. nov.

Pseudomonas silesiensis (si.le.si.en'sis. N.L. adj. *silesiensis*) pertains to Silesia, a southwestern district of Poland where the strain was first isolated.

Cells from this strain stain Gram-negative are rod-shaped (0.8 µm wide, 3 µm long), motile with single polar flagellum, and oxidase positive. Colonies grown on LB medium are round shape, smooth surface and edges, and exhibit a milky-yellow color. Growth occurs in 0-4 % (w/v) NaCl, at pH from 6 to 9 (optimum 7-8) and at a temperature of 4-35°C (optimum 15-30°C). The strain is ampicillin resistant up to the tested concentration of 400 µg/mL. In API 20 NE test nitrate reduction to nitrites is positive. Nitrite reduction as well as indole production, glucose fermentation, arginine dihydrolase, urease, β-glucosidase, protease and β-galactosidase activities are negative. Assimilation of D-glucose, L-arabinose, D-mannose, D-mannitol, D-maltose, potassium gluconate, capric acid and malic acid is positive. Negative results were obtained for utilization of N-acetyl-glucosamine, adipic acid, trisodium citrate and phenylacetic acid. Plate test analysis performed using the Biolog System GENIII platform indicated that the A3^T strain has the ability to oxidize a variety of carbon sources: D-trehalose, sucrose, α-D-glucose, D-mannose, D-fructose, D-galactose, D-sorbitol, D-mannitol, D-arabitol, glycerol, L-alanine, L-arginine, L-aspartic acid, L-glutamic acid, L-histidine, L-pyroglutamic

acid, L-serine, pectin, D-galacturonic acid, L-galactonic acid lactone, D-gluconic acid, D-glucuronic acid, glucuronamide, mucic acid, quinic acid, D-saccharic acid, methyl pyruvate, L-lactic acid, citric acid, α-keto-glutaric acid, D-malic acid, L-malic acid, bromo-succinic acid, tween 40, γ-amino-butyric acid, α-hydroxy-butyric acid, β-hydroxy-D,L-butyric acid, acetoacetic acid, propionic acid and acetic acid. This strain does not oxidize the following substrates: D-maltose, D-cellobiose, gentiobiose, D-turanose, stachyose, D-raffinose, α-D-lactose, D-melibose, β-methyl-D-glucoside, D-scilicin, N-acetyl-D-glucosamine, N-acetyl-β-D-mannosamine, N-acetyl-D-galactosamine, N-acetyl-neuraminic acid, 3-methyl glucose, L-rhamnose, myo-inositol, D-aspartic acid, gelatin, D-lactic acid methyl ester. Weak results were observed for: D-fucose, inosine, D-serine, D-fructose-6-PO_4, D-serine, glycyl-L-proline, nalidixic acid, α-keto-butyric acid and formic acid. Variable results were observed for dextrin, L-fucose, p-hydroxyphenyl acetic acid and D-glucose-6-PO_4. In Biolog GENIII plates the $A3^T$ strain showed resistance to: aztreonam, 1% sodium lactate, potassium tellurite, fusudic acid, troleandomycin, rifamycin SV, vancomycin and sodium bromate, whereas vulnerable for: minocycline, lithium chloride and sodium butyrate.

The predominant cellular fatty acids include summed feature 3, $C_{16:0}$ and $C_{18:1\ \omega7c}$. G+C base composition is 59.58 mol%. Regarding all phenotypic tests performed, strain $A3^T$ (=PCM 2856^T =DSM 103370^T) could be differentiated form other species belonging to the *P. mandelii* subgroup type strains by a lack of N-acetyl-D-glucosamine and myo-inositol oxidizing ability and the lack of growth in the presence of minocycline, N-acetyl-D-glucosamine and trisodium citrate. The type strain $A3^T$ was isolated from a subsurface flow constructed wetland of a wastewater treatment plant operated by pesticide producer in Jaworzno City, Poland. Digital Protologue Taxonumber: TA00122.

Competing interests

The authors declare that the research was conducted in the absence of any commercial or financial relationships that could be construed as a potential conflict of interest.

Funding Acknowledgements

This work was supported by the European Union's European Regional Development Fund through the Innovative Economy Operational Program, 2007–2013 (project support agreement POIG.01.01.02-14-054/09-00).

Authors' contributions

L.L, A.S. conceived and directed the studies. M.A.K., E.M.F. participated in bacteria isolation form soil and phenotype analysis. DNA isolation, DNA libraries preparation, genome sequencing and all bioinformatics analysis was performed by. M.A.K. The manuscript was written by M.A.K., consulted and corrected by L.L., A.S., A.D. Funding for this work was provided by L.L. and A.D. All authors read and approved the final manuscript.

Acknowledgements

We are grateful to dr Andrzej Silowiecki from Institute of Plant Protection, National Research Institute, Sosnicowice branch for help and support in sample collection. Electron microscopy was performed by Electron Microscopy Platform in Mossakowski Medical Research Centre PAS. All type strains of closely related species to *P. silesiensis sp. nov.* A3^T used in this study were purchased from Leibniz Institute DSMZ-German Collection of Microorganisms and Cell Cultures.

References

1. Oren A, Garrity GM. Then and now: A systematic review of the systematics of prokaryotes in the last 80 years. Antonie van Leeuwenhoek, Int J Gen Mol Microbiol. 2014;106:43–56.
2. Mulet M, Lalucat J, García-Valdés E. DNA sequence-based analysis of the Pseudomonas species. Environ Microbiol. 2010;12:1513–30.
3. Garrido-Sanz D, Meier-Kolthoff JP, Göker M, Martín M, Rivilla R, Redondo-Nieto M. Genomic and Genetic Diversity within the Pseudomonas fluorescens Complex. PLoS One. 2016;11:e0150183.
4. Albuquerque MGE, Martino V, Pollet E, Avérous L, Reis MAM. Mixed culture polyhydroxyalkanoate (PHA) production from volatile fatty acid (VFA) -rich streams : Effect of substrate composition and feeding regime on PHA productivity , composition and properties. J Biotechnol. Elsevier B.V.; 2011;151:66–76.
5. Liu W, Chen G. Production and characterization of medium-chain-length

polyhydroxyalkanoate with high 3-hydroxytetradecanoate monomer content by fadB and fadA knockout mutant of Pseudomonas putida KT2442. Appl Microbiol Biotechnol. 2007;1153–9.

6. Prakash D, Pandey J, Tiwary BN, Jain RK. A process optimization for bio-catalytic production of substituted catechols (3-nitrocatechol and 3-methylcatechol). BMC Biotechnol. 2010;10:1–9.

7. Martin CH, Wu D, Prather KLJ. Integrated Bioprocessing for the pH-Dependent Production of 4-Valerolactone from Levulinate in Pseudomonas putida KT2440. Appl Env Microbiol. 2010;76:417–24.

8. Graf N, Altenbuchner J. Genetic engineering of Pseudomonas putida KT2440 for rapid and high-yield production of vanillin from ferulic acid. Appl Microbiol Biotechnol. 2014;137–49.

9. Poblete-Castro I, Becker J, Dohnt K. Industrial biotechnology of Pseudomonas putida and related species. Appl Microbiol Biotechnol. 2012;2279–90.

10. Álvarez MS, Rodríguez A, Sanromán MÁ, Deive FJ. Bioresource Technology Simultaneous biotreatment of Polycyclic Aromatic Hydrocarbons and dyes in a one-step bioreaction by an acclimated Pseudomonas strain. 2015;198:181–8.

11. Chaturvedi V, Kumar A. Isolation of a strain of Pseudomonas putida capable of metabolizing anionic detergent sodium dodecyl sulfate (SDS). Iran J Microbiol. 2011;1:47–53.

12. Limcharoensuk T, Sooksawat N, Sumarnrote A, Awutpet T, Kruatrachue M, Pokethitiyook P, et al. Ecotoxicology and Environmental Safety Bioaccumulation and biosorption of Cd 2 þ and Zn 2 þ by bacteria isolated from a zinc mine in Thailand. Ecotoxicol Environ Saf. Elsevier; 2015;122:322–30.

13. Wasi S, Tabrez S, Ahmad M. Use of Pseudomonas spp. for the bioremediation of environmental pollutants : a review. 2013;8147–55.

14. Younas A, Hilber I, Rehman S. Former DDT factory in Pakistan revisited for remediation : severe DDT concentrations in soils and plants from within the area. Env Sci Pollut Res. 2013;1966–76.

15. Mishra K, Sharma RC, Kumar S. Ecotoxicology and Environmental Safety Contamination levels and spatial distribution of organochlorine pesticides in soils from India. Ecotoxicol Environ Saf. Elsevier; 2012;76:215–25.

16. Lal R, Pandey G, Sharma P, Kumari K, Malhotra S, Pandey R, et al. Biochemistry of microbial degradation of hexachlorocyclohexane and prospects for bioremediation. Microbiol Mol Biol Rev. 2010 Mar;74:58–80.

17. Sharma P, Raina V, Kumari R, Malhotra S, Dogra C, Kumari H, et al. Haloalkane dehalogenase LinB is responsible for beta- and delta-hexachlorocyclohexane transformation in Sphingobium indicum B90A. Appl Environ Microbiol. 2006 Sep;72:5720–7.

18. Verhille S, Baida N, Dabboussi F, Izard D, Leclerc H. Taxonomic study of bacteria isolated from natural mineral waters: proposal of Pseudomonas jessenii sp. nov. and Pseudomonas mandelii sp. nov. Syst Appl Microbiol. 1999 Feb;22:45–58.

19. Jang S-H, Kim J, Kim J, Hong S, Lee C. Genome Sequence of Cold-Adapted Pseudomonas mandelii Strain JR-1. J Bacteriol. 2012 Jun 15;194:3263–3263.

20. Verhille S, Baïda N, Dabboussi F, Hamze M, Izard D, Leclerc H. Pseudomonas gessardii sp. nov. and Pseudomonas migulae sp. nov., two new species isolated from natural mineral waters. Int J Syst Bacteriol. 1999 Oct;49 Pt 4:1559–72.

21. Delorme S, Lemanceau P, Christen R, Corberand T, Meyer JM, Gardan L. Pseudomonas lini sp. nov., a novel species from bulk and rhizospheric soils. Int J Syst Evol Microbiol. 2002;52:513–23.

22. Campos VL, Valenzuela C, Yarza P, Kampfer P, Vidal R, Zaror C, et al. Pseudomonas arsenicoxydans sp nov., an arsenite-oxidizing strain isolated from the Atacama desert. Syst

Appl Microbiol. 2010;33:193–7.

23. Andersen SM, Johnsen K, Sørensen J, Nielsen P, Jacobsen CS. Pseudomonas frederiksbergersis sp. nov., isolated from soil at a coal gasification site. Int J Syst Evol Microbiol. 2000;50:1957–64.

24. Dudášová H, Lukáčová L, Murínová S, Puškárová A, Pangallo D, Dercová K. Bacterial strains isolated from PCB-contaminated sediments and their use for bioaugmentation strategy in microcosms. J Basic Microbiol. 2014 Apr;54:253–60.

25. Zhou J, Bruns MA, Tiedje JM. DNA recovery from soils of diverse composition. Appl Environ Microbiol. 1996 Feb;62:316–22.

26. Bennasar A, Mulet M, Lalucat J, García-Valdés E. PseudoMLSA: a database for multigenic sequence analysis of Pseudomonas species. BMC Microbiol. 2010;10:118.

27. Tamura K, Stecher G, Peterson D, Filipski A, Kumar S. MEGA6: Molecular Evolutionary Genetics Analysis Version 6.0. Mol Biol Evol. 2013 Dec 1;30:2725–9.

28. Tamura K, Nei M. Estimation of the number of nucleotide substitutions in the control region of mitochondrial DNA in humans and chimpanzees. Mol Biol Evol. 1993 May;10:512–26.

29. Heimbrook ME, Wang WENLANL, Campbell G. Staining Bacterial Flagella Easily. J Clin Microbiol. 1989;27:2612–5.

30. Spiekermann P, Rehm BHA, Kalscheuer R, Baumeister D, Steinbüchel A. A sensitive, viable-colony staining method using Nile red for direct screening of bacteria that accumulate polyhydroxyalkanoic acids and other lipid storage compounds. Arch Microbiol. 1999;171:73–80.

31. Martin M. Cutadapt removes adapter sequences from high-throughput sequencing reads. EMBnet.journal. 2011;17:10.

32. Joshi N, Fass J. Sickle: A sliding-window, adaptive, quality-based trimming tool for FastQ files [Internet]. 2011. Available from: https://github.com/najoshi/sickle

33. Bankevich A, Nurk S, Antipov D, Gurevich AA, Dvorkin M, Kulikov AS, et al. SPAdes: A New Genome Assembly Algorithm and Its Applications to Single-Cell Sequencing. J Comput Biol. 2012;19:455–77.

34. Angiuoli SV, Gussman A, Klimke W, Cochrane G, Field D, Garrity GM, et al. Toward an Online Repository of Standard Operating Procedures (SOPs) for (Meta)genomic Annotation. Omi A J Integr Biol. 2008 Jun;12:137–41.

35. Petersen TN, Brunak S, von Heijne G, Nielsen H. SignalP 4.0: discriminating signal peptides from transmembrane regions. Nat Methods. 2011 Sep 29;8:785–6.

36. Saier MH, Tran CV, Barabote RD. TCDB: the Transporter Classification Database for membrane transport protein analyses and information. Nucleic Acids Res. 2006;34:D181-6.

37. Yoon S, Ha S, Kwon S, Lim J, Kim Y, Seo H, et al. Introducing EzBioCloud : a taxonomically united database of 16S rRNA gene sequences and whole-genome assemblies. 2017;67:1613–7.

38. Richter M, Rosselló-Móra R, Oliver Glöckner F, Peplies J. JSpeciesWS: a web server for prokaryotic species circumscription based on pairwise genome comparison. Bioinformatics. 2016 Mar 15;32:929–31.

39. Meier-Kolthoff JP, Auch AF, Klenk H-P, Göker M. Genome sequence-based species delimitation with confidence intervals and improved distance functions. BMC Bioinformatics. 2013;14:60.

40. Palleroni N. Pseudomonas. Bergey's Man Syst Archaea Bact. 2015;

41. Redondo-Nieto M, Barret M, Morrissey J, Germaine K, Martínez-Granero F, Barahona E, et al. Genome sequence reveals that Pseudomonas fluorescens F113 possesses a large and diverse array of systems for rhizosphere function and host interaction. BMC Genomics. 2013;14:54.

42. Lopez N, Pettinari MJ, Nikel PI, Méndez BS. Polyhydroxyalkanoates : Much More than Biodegradable Plastics. Adv Appl Microbiol. 2015;93:73–106.
43. Li R, Jiang Y, Wang X, Yang J, Gao Y, Zi X, et al. Psychrotrophic Pseudomonas mandelii CBS-1 produces high levels of poly-β-hydroxybutyrate. Springerplus. 2013;2:335.
44. Rehm BH. Polyester synthases: natural catalysts for plastics. Biochem J. 2003;376:15–33.
45. Ates O. Systems Biology of Microbial Exopolysaccharides Production. Front Bioeng Biotechnol. 2015 Dec 18;3.
46. Römling U, Galperin MY. Bacterial cellulose biosynthesis: Diversity of operons, subunits, products, and functions. Trends Microbiol. 2015;23:545–57.
47. Karp PD, Paley SM, Krummenacker M, Latendresse M, Dale JM, Lee TJ, et al. Pathway Tools version 13.0: integrated software for pathway/genome informatics and systems biology. Brief Bioinform. 2010;11:40–79.
48. Liu R, Ochman H. Origins of flagellar gene: Operons and secondary flagellar systems. J Bacteriol. 2007;189:7098–104.
49. Dhillon BK, Laird MR, Shay JA, Winsor GL, Lo R, Nizam F, et al. IslandViewer 3: more flexible, interactive genomic island discovery, visualization and analysis. Nucleic Acids Res. 2015;43:W104–8.
50. Field D, Garrity G, Gray T, Morrison N, Selengut J, Sterk P, et al. The minimum information about a genome sequence (MIGS) specification. Nat Biotechnol. 2008;26:541–7.
51. Field D, Amaral-Zettler L, Cochrane G, Cole JR, Dawyndt P, Garrity GM, et al. The Genomic Standards Consortium. PLoS Biol. 2011;9:e1001088.
52. Woese CR, Kandler O, Wheelis ML. Towards a natural system of organisms: proposal for the domains Archaea, Bacteria, and Eucarya. Proc Natl Acad Sci U S A. 1990 Jun;87:4576–9.
53. Garrity GM, Brenner DJ, Krieg NR, Staley JR. The Proteobacteria. Bergey's Man Syst Bacteriol. 2005;
54. Garrity G, Brenner DJ, Krieg NR, Staley JR. The Proteobacteria, Part B: The Gammaproteobacteria. Bergey's Man Syst Bacteriol. 2005;2.
55. Williams KP, Kelly DP. Proposal for a new class within the phylum Proteobacteria, Acidithiobacillia classis nov., with the type order Acidithiobacillales, and emended description of the class Gammaproteobacteria. Int J Syst Evol Microbiol. 2013 Aug;63:2901–6.
56. Sneath PHA, McGowan V, Skerman VBD. Approved Lists of Bacterial Names. Int J Syst Evol Microbiol. 1980 Jan 1;30:225–420.
57. Orla-Jensen S. The Main Lines of the Natural Bacterial System. J Bacteriol. 1921 May;6:263–73.
58. Winslow CE, Broadhurst J, Buchanan RE, Krumwiede C, Rogers LA, Smith GH. The Families and Genera of the Bacteria: Preliminary Report of the Committee of the Society of American Bacteriologists on Characterization and Classification of Bacterial Types. J Bacteriol. 1917 Sep;2:505–66.
59. Migula W. Über ein neues System der Bakterien. Arb aus dem Bakteriol Inst der Tech Hochschule zu Karlsruhe. 1894;1:235–8.
60. Ashburner M, Ball CA, Blake JA, Botstein D, Butler H, Cherry JM, et al. Gene ontology: tool for the unification of biology. The Gene Ontology Consortium. Nat Genet. 2000 May;25:25–9.
61. Bose T, Haque MM, Reddy C, Mande SS. COGNIZER : A Framework for Functional Annotation of Metagenomic Datasets. PLoS One. 2015;10:1–16.
62. Alikhan N-F, Petty NK, Ben Zakour NL, Beatson SA. BLAST Ring Image Generator (BRIG): simple prokaryote genome comparisons. BMC Genomics. 2011;12:402.

Table 1. Classification and the general and genomic features of *Pseudomonas silesiensis* strain A3^T according to the MIGS (Minimum Information about a Genome Sequence) recommendation [50] published by The Genomic Standards Consortium [51].

MIGS ID[a]	Property	Term	Evidence code[b]
	Classification	Domain *Bacteria*	TAS [52]
		Phylum *Proteobacteria*	TAS [53]
		Class *Gammaproteobacteria*	TAS [54,55]
		Order *Pseudomonadales*	TAS [56,57]
		Family *Pseudomonadaceace*	TAS [56,58]
		Genus *Pseudomonas*	TAS [56,59]
		Species *Pseudomonas silesiensis*	TAS [this study]
		strain: *A3^T*	IDA
	Gram stain	*Negative*	IDA
	Cell shape	*Rod*	IDA
	Motility	*Motile*	IDA
	Sporulation	*Negative*	IDA
	Temperature range	*4-35°C*	IDA
	Optimum temperature	*15-30°C*	IDA
	pH range; Optimum	*Range 6.0-9.0; Optimum 7.0-8.0*	IDA
	Carbon source	*Wide range of organic carbon substrates*	IDA
MIGS-6	Habitat	*Pesticide production factory associated wastewater treatment plant*	IDA
MIGS-6.3	Salinity	*0-4% NaCl*	IDA
MIGS-22	Oxygen requirement	*Aerobic*	IDA
MIGS-15	Biotic relationship	*Free-living*	IDA
MIGS-14	Pathogenicity	*Non-pathogen*	NAS
MIGS-4	Geographic location	*Poland; Jaworzno*	IDA
MIGS-5	Sample collection	*14 July 2010*	IDA
MIGS-4.1	Latitude	*50°12'54.0"N*	IDA
MIGS-4.2	Longitude	*19°14'03.0"E*	IDA
MIGS-4.4	Altitude	*263.04 m*	IDA
MIGS 31	Genome quality status	Finished	
MIGS 28	Libraries used	500bp, 8kb, 20kb	
MIGS 29	Sequencing platform	Ilumina	
MIGS 31.2	Fold coverage	95x	
MIGS 30	Assemblers	SPAdes 3.6.2	
MIGS 32	Gene calling method	GeneMarkS+	
	Locus Tag	PMA3	
	GenBank ID	CP014870.1	
	GenBank Date of Release	10-06-2016	
	GOLD ID	GP0137126	
	BIOPROJECT	PRJNA315635	
MIGS 13	Source Material Identifier	SAMN04566726	
	Project relevance	Bioremediation	

[a] Evidence codes - IDA: Inferred from Direct Assay; TAS: Traceable Author Statement (i.e., a direct report exists in the literature); NAS: Non-traceable Author Statement (i.e., not directly observed for the living, isolated sample, but based on a generally accepted property for the species, or anecdotal evidence). These evidence codes are from the Gene Ontology project [60].

Table 2. Genome sequence similarity between *P. silesiensis* A3^T and genome sequences of closely related type strains with sequenced genomes. All the bioinformatic methods used indicate significant separation of the A3^T strain as a separate species.

Strains	ANIb (%)	dDDH (%)	Tetra z-score
P. arsenicoxydans CECT 7543^T	85.63	33.30	0.98469
P. lini DSM 16768^T	85.93	34.00	0.97928
P. mandelii LMG 21607^T	**86.31**	**34.50**	**0.98344**
P. tremae ICMP 9151^T	76.33	22.90	0.92139
P.cannabina ICMP 2823^T	76.85	23.10	0.93837
P. meliae CFBP 3225^T	76.75	22.90	0.91281

The highest values among the selected genomes are shown in bold.

Table 3. Differential characteristics of *P. silesiensis* A3^T and its phylogenetically closest related species.

Features	1	2	3	4	5
GC content (%)	59.6	59.6[‡]	58.7[¥]	58.4[†]	57.0[§]
Flagellation	Single polar flagellum	Single polar flagellum[‡]	Multiple polar flagella[¤]	Multiple polar flagella[†]	Single polar flagellum[§]
Salt tolerance range (% w/v)	0.0-4.0	0.0-4.0	0.0-4.0	0.0-4.0	0.0-5.0
Fluorescence on King B medium	-	-	-	+	+
Agrinine dihydrolase activity [1]	-	-	+	-	-
Minocycline sensitivity [2]	-	+	+	+	+
Nitrates reduction ability to [1]:	Nitrites	Nitrogen	-	Nitrites	Nitrites
Oxidation of:					
D-sorbitol [2]	+	-	+	+	+
Myo-Inositol [2]	-	+	-	+	+
Assimilation of:					
N-acetyl-D-glucosamine [1]	-	+	+	+	+
D-Maltose [1]	+	-	+	-	-
Trisodium citrate [1]	-	+	+	+	+

Lanes: 1, *P. silesiensis* A3^T; 2, *P. frederiksbergensis* DSM 13022^T; 3, *P. arsenicoxydans* DSM 27171^T; 4, *P. lini* DSM 16768^T; 5, *P. mandelii* DSM 17967^T.

[1] - result from API 20NE test,

[2] – result from Biolog GEN III test. Data were obtained in this study unless specifically indicated.

+, positive; -, negative.

[‡]Andersen et al. (2000)[23]

[¥]Calculated from genome sequence LT629705.1.

[¤]Campos et al. (2010)[22]

[†]Delorme et al. (2002)[21]

[§]Verhille et al. (1999)[18]

Table 4. Cellular fatty acid composition (%) derived from FAME analysis of *Pseudomonas silesiensis* sp. nov. A3^T and the type strains of closely related *Pseudomonas* species. All strains were tested in the same culture conditions described in the **Materials and Methods** section.

Fatty acid	1	2	3	4	5
$C_{10:0\ 3OH}$	3.7	3.8	5.7	4.1	4.2
$C_{12:0}$	6.5	2.1	2.5	4.8	5.2
$C_{12:0\ 2OH}$	1.0	4.1	4.6	2.5	2.3
$C_{12:0\ 3OH}$	3.1	4.3	6.5	4.1	3.9
$C_{12:1\ 3OH}$	0.2	0.2	4.0	0.5	0.1
Summed feature 3*	36.9	34.0	34.2	36.4	36.9
$C_{16:0}$	27.9	32.1	28.9	25.8	33.7
$C_{17:0\ cyclo}$	1.0	5.4	1.5	1.0	3.1
$C_{18:1\ \omega7c}$	18.3	11.9	9.3	19.2	9.2

Lanes: 1, *P. silesiensis* A3^T; 2, *P. arsenicoxydans* DSM 27171^T; 3, *P.frederiksbergensis* DSM 13022^T; 4, *P. lini* DSM 16768^T; 5, *P. mandelii* DSM 17967^T.

*Summed features represent a set of more than one fatty acid that could not be resolved with the MIDI system. Summed feature 3 contained $C_{16:1\ \omega7c}$ and/or $C_{15:0\ ISO\ 2OH}$.

Table 5. General statistics of *P. silesiensis* A3^T genome.

Attribute	Value	% of Total
Genome size (bp)	6,823,539	100.0
DNA coding (bp)	5,599,458	82.06
DNA G+C (bp)	4,065,634	59.58
Total genes	6,066	100
Protein coding genes	5,875	96.85
RNA genes	96	1.58
Pseudo genes	95	1.57
Genes with function prediction	4,792	78.99
Genes assigned to COGs	4,362	71.90
Genes with Pfam domains	4,358	71.84
Genes with signal peptides	641	10.56
Genes with transmembrane helices	1,318	21.72

Table 6. Comparison of gene counts associated with the general COGs (Clusters of Orthologous Groups) functional categories for genomes of *P. silesiensis* A3^T, *P. mandelii* LMG 21607^T, *P. lini* DSM 16768^T and *P. arsenicoxydans* CECT 7543^T. Association of genes to COG categories for each genome was done using COGNIZER software [61].

		P. silesiensis A3^T		*P. mandelii* LMG 21607^T		*P. lini* DSM 16768^T		*P. arsenicoxydans* CECT 7543^T	
Code	**Description**	**Value**	**%age**	**Value**	**%age**	**Value**	**%age**	**Value**	**%age**
J	**Translation, ribosomal structure and biogenesis**	314	3,31%	307	3,12%	299	3,30%	299	3,24%
A	**RNA processing and modification**	1	0,01%	1	0,01%	1	0,01%	1	0,01%
K	**Transcription**	739	7,78%	756	7,69%	683	7,55%	687	7,44%
L	**Replication, recombination and repair**	328	3,45%	458	4,66%	310	3,43%	391	4,24%
B	**Chromatin structure and dynamics**	6	0,06%	5	0,05%	6	0,07%	4	0,04%
D	**Cell cycle control, cell division, chromosome partitioning**	58	0,61%	62	0,63%	61	0,67%	64	0,69%
V	**Defense mechanisms**	144	1,52%	162	1,65%	150	1,66%	153	1,66%
T	**Signal transduction mechanisms**	619	6,52%	739	7,51%	628	6,94%	722	7,82%
M	**Cell wall/membrane/envelope biogenesis**	456	4,80%	535	5,44%	507	5,60%	502	5,44%
N	**Cell motility**	192	2,02%	226	2,30%	207	2,29%	227	2,46%
U	**Intracellular trafficking, secretion, and vesicular transport**	160	1,68%	183	1,86%	195	2,16%	163	1,77%
O	**Posttranslational modification, protein turnover, chaperones**	305	3,21%	305	3,10%	290	3,21%	291	3,15%
C	**Energy production and conversion**	701	7,38%	614	6,24%	580	6,41%	607	6,58%
G	**Carbohydrate transport and metabolism**	534	5,62%	583	5,93%	565	6,24%	555	6,01%
E	**Amino acid transport and metabolism**	1218	12,82%	1118	11,37%	1074	11,87%	1125	12,19%
F	**Nucleotide transport and metabolism**	170	1,79%	167	1,70%	154	1,70%	181	1,96%
H	**Coenzyme transport and metabolism**	314	3,31%	302	3,07%	288	3,18%	298	3,23%
I	**Lipid transport and metabolism**	445	4,68%	428	4,35%	383	4,23%	375	4,06%
P	**Inorganic ion transport and metabolism**	655	6,89%	693	7,05%	595	6,58%	607	6,58%
Q	**Secondary metabolites biosynthesis, transport and catabolism**	325	3,42%	337	3,43%	329	3,64%	239	2,59%
R	**General function prediction only**	1204	12,67%	1247	12,68%	1109	12,26%	1146	12,41%
S	**Function unknown**	612	6,44%	608	6,18%	634	7,01%	594	6,43%

Figure legends

Figure 1. Images of *Pseudomonas silesiensis* strain A3^T colonies grown on an LB solid medium at 23°C for 2 days (A), bacterial morphology obtained from optical microscopy with 160x magnification showing single polar flagellum after staining (B) and transmission electron microscopy (C). White arrows indicate single polar flagellum (B) and PHA granules (C).

Figure 2. Phylogenetic tree of type strains closely related to *Pseudomonas silesiensis* A3^T (in bold) belonging to the *Pseudomonas fluorescens* group based on 16S rRNA gene sequence. All positions containing gaps or missing data were excluded, which resulted in a 1,271 bp sequence in the final dataset. Bootstrap values are represented at the branching points (only values >50% are shown). The bar represents 0.005 substitutions per site.

Figure 3. Phylogenetic tree constructed using concatenated partial sequences of 16S rRNA, *gyrB*, *rpoD* and *rpoB* genes representing the relative position of *Pseudomonas silesiensis* strain A3^T (in bold) in the *Pseudomonas* genus. All positions containing gaps or missing data were excluded. The final dataset contained 3,345 positions. Accession numbers of sequences used in this study are listed in Supplementary table 1. Bootstrap values are represented at the branching points (only values >50% are shown). *Gene sequences for *P. silesiensis* A3^T were retrieved directly from the genome (CP014870.1). The bar represents 0.05 substitutions per site.

Figure 4. Genomic representation of the *Pseudomonas silesiensis* A3^T genome. Rings from inside: 1 – GC content, ring 2 – GC skew, ring 3 – tRNA genes, ring 4 – rRNA genes, rings 5-7 – genomic sequence identity at minimum 80% similarity with genomes of closely related type strains of *P. mandelii* LMG 21607^T, *P. lini* DSM 16768^T and *P. arsenicoxydans* CECT 7543^T. Figure prepared using BRIG software [62].

Figure
Click here to download high resolution image

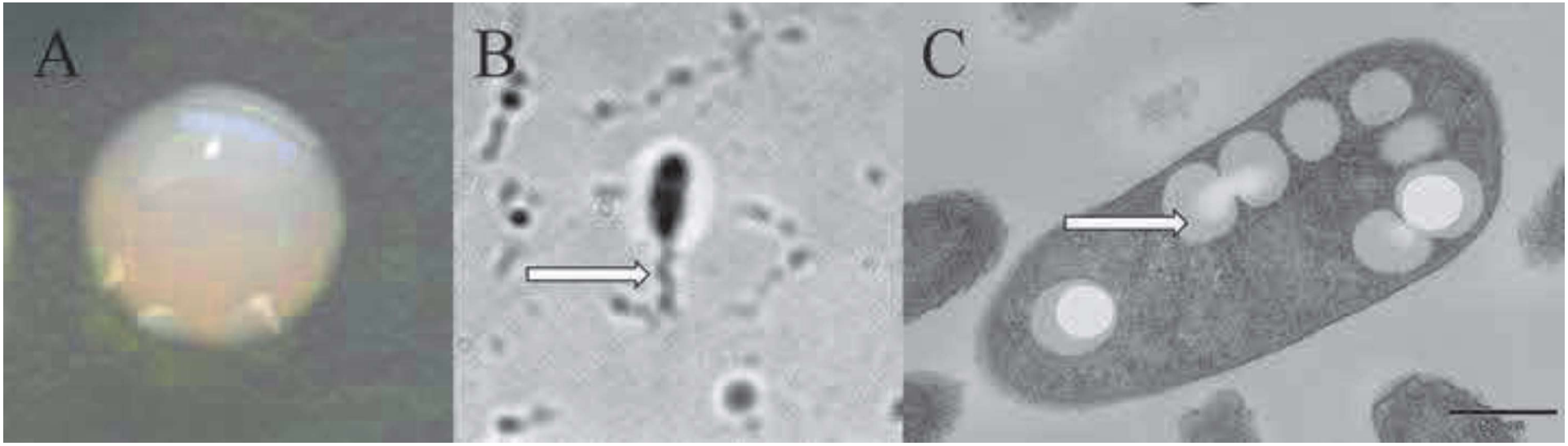

Figure 2

Click here to download high resolution image

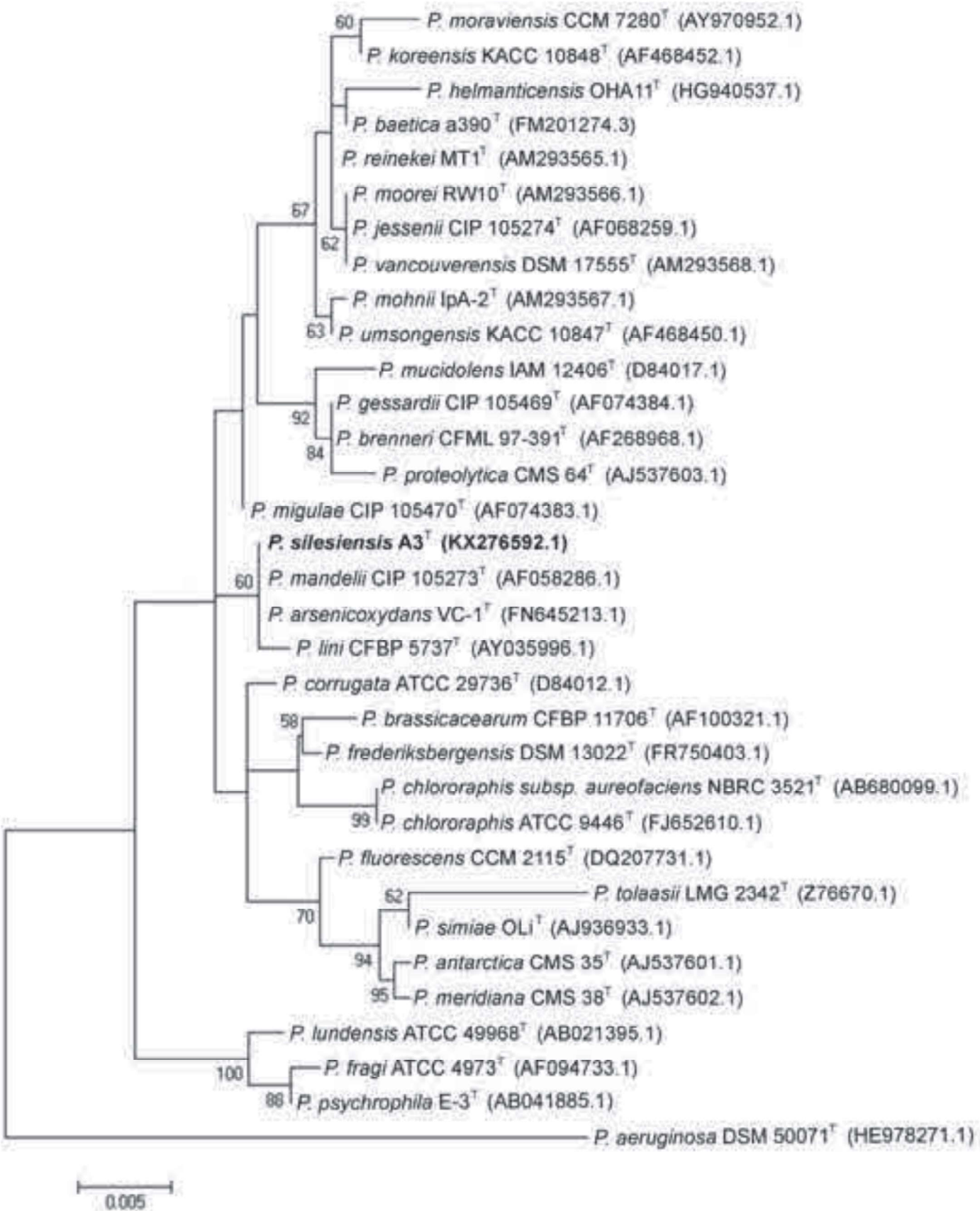

Figure 3

Click here to download high resolution image

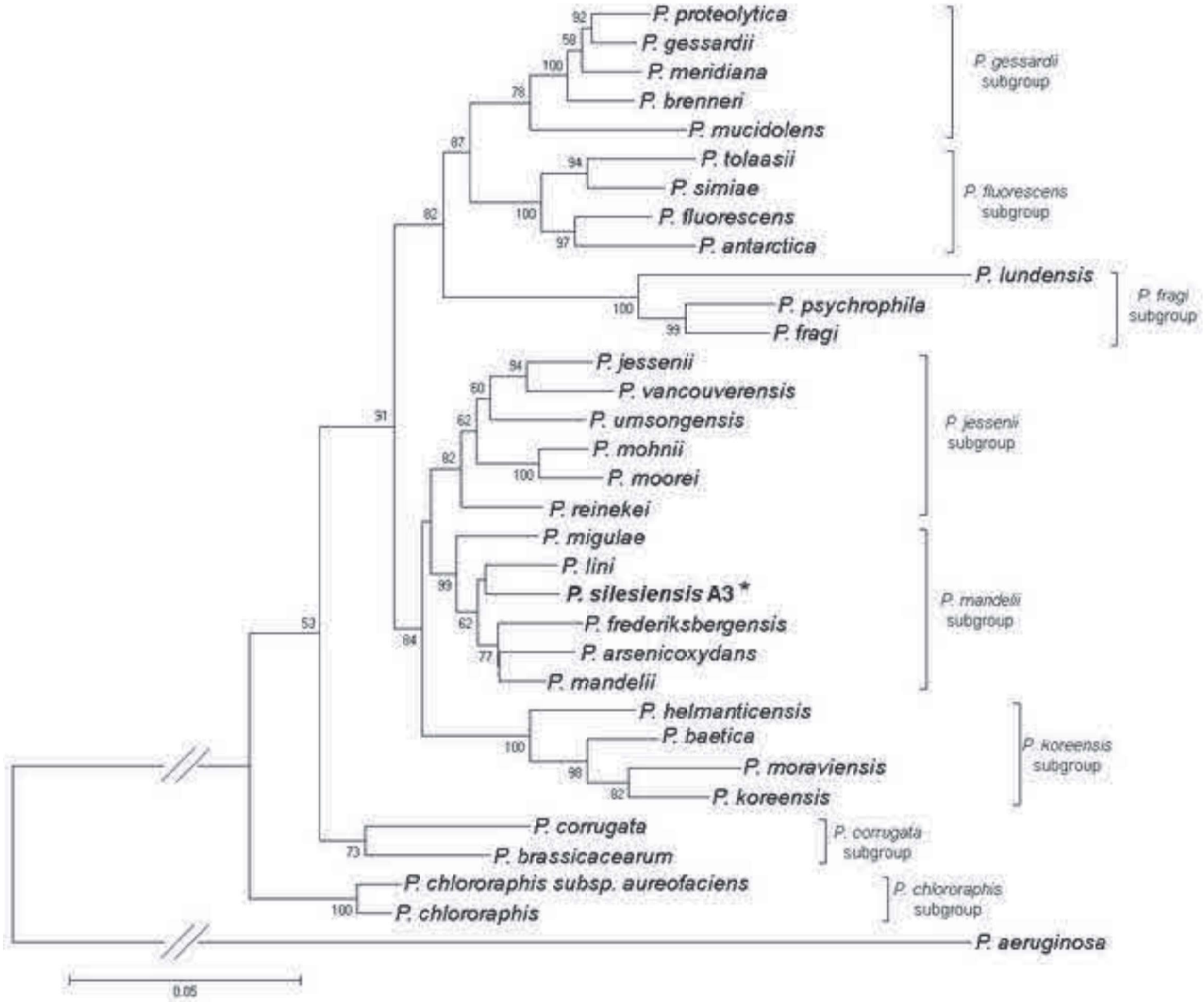

Figure 4

Click here to download high resolution image